

地质样品 Nd 同位素激光原位等离子体质谱 (LA-MC-ICPMS) 测定

杨岳衡, 孙金凤, 谢烈文, 范宏瑞, 吴福元*

中国科学院地质与地球物理研究所, 岩石圈演化国家重点实验室, 北京 100029

* 联系人, E-mail: wufuyuan@mail.igcas.ac.cn

2007-11-23 收稿, 2008-01-14 接受

国家自然科学基金资助项目(批准号: 40773008, 40325006)

摘要 利用配有 193 nm 激光的 Neptune 多接收等离子体质谱仪(MC-ICPMS), 采用最新发表的 Sm 同位素丰度和本研究中测定的 Sm 和 Nd 之间的质量歧视关系, 对磷灰石、榍石、独居石和钙钛矿等天然矿物进行了一系列微区原位 Nd 同位素测定. 结果表明, 大量 Ce 的存在不会影响 Nd 同位素的精确与准确测定, 在 $Sm/Nd < 1$ ($^{147}Sm/^{144}Nd < 0.6$) 范围内, 建立的方法可以准确获得足够 Nd 含量地质样品的 Nd 同位素组成. 结合其微量元素和 U-Pb 年龄, 激光 Nd 同位素资料可为精细地质作用过程的探讨提供重要信息.

关键词

Nd 同位素

磷灰石

榍石

独居石

钙钛矿

LA-MC-ICPMS

Nd同位素是地球化学和地质年代学的重要组成部分, 是探讨岩石成因和壳幔演化最重要的示踪手段之一^[1]. 目前广泛采用的Nd同位素测定方法是, 首先通过化学方法使得样品溶解, 然后进行至少 2 次离子交换分离等纯化手段, 使得Sm与Nd彻底分开, 最后用热电离质谱(Thermal ionization mass spectrometry, TIMS) 对得到的纯净Nd组分进行质谱测试^[2], 从而获得研究对象的Nd同位素组成. 但近年来, 同位素地球化学领域出现两个显著的进展. 其一是多接收等离子质谱(multiple collector inductively coupled plasma mass spectrometry, MC-ICPMS)被广泛应用于各种同位素的测定^[3,4]. 就Nd同位素而言, 运用MC-ICPMS仪器可以获得与TIMS精度相媲美的数据^[5-9]. 但和前述的TIMS一样, 它们采用的均是整体分析(bulk analysis), 所获得的数据是所研究样品不同组成部分Nd同位素的平均值. 由于地质过程的复杂性, 天然矿物大多存在一定的成分环带, 从而导致获取天然矿物内部同位素成分的变化成为当前同位素地球化学研究最重要的研究进展和前沿领域, 如离子探针和激光探针在矿物微区原位(*in situ*)同位素分析上的广泛运用等. 由于

MC-ICPMS的离子源处于常压之下, 我们可以非常方便地改变其进样方式, 从而导致目前MC-ICPMS与激光剥蚀(Laser ablation, LA)系统实现广泛的联用, 实现矿物微区的原位同位素分析. 该方法不仅揭示了常规整体分析所掩盖的细微空间变化的重要信息, 同时也避免了冗长繁琐的化学处理, 效率明显提高. 因此, 该方法目前已被广泛用于Sr, Hf, Os, B和Mg等同位素测定中^[10], 为大量重要地质问题的讨论提供了重要资料. 但相对而言, Nd同位素的激光原位测定目前开展得较少. 其主要原因是由于Sm对Nd同位素测定的干扰. 尽管如此, 最近两年来, 部分国外学者对这一问题进行了有益的探索^[11-13], 就磷灰石、榍石、铁锰结核、独居石、褐帘石等天然矿物获得了较为可信的Nd同位素资料, 显示了这一技术潜在的研究价值. 但由于该方法的开发还处于初步发展阶段, 许多重要问题仍未获得解决. 在这一背景下, 本文利用中国科学院地质与地球物理研究所引进的Neptune MC-ICPMS和193 nm激光取样系统, 对Nd同位素的激光原位测定方法进行了全面探讨, 并对磷灰石、榍石、独居石和钙钛矿等天然矿物进行了微区原位Nd同位素测定, 获得

了非常理想的测定结果.

1 仪器简介

Nd同位素测定是在中国科学院地质与地球物理研究所引进的Neptune MC-ICPMS和 193 nm 准分子激光系统上进行的. 其中Neptune MC-ICPMS仪器的基本情况已在相关文献中作过详细介绍 [14,15].

GeoLas Plus 型紫外激光剥蚀系统是在 GeoLas CQ 型基础上的升级产品, 德国 Lambda Physik 公司制造, 该系统主要包括: () Compex 102型 ArF 准分子激光发生器, 激光波长为 193 nm, 激光脉冲宽度 15 ns, 脉冲输出能量最高为 200 mJ; () GeoLas 公司设计的激光匀化光路系统, 匀化器透镜单元组为 13×13, 激光束斑大小为 4, 10, 20, 30, 40, 50, 60, 70, 80, 90, 100, 110, 120, 130 和 160 μm 可调, 脉冲速率为 1~20 Hz 连续可调; () GeoLas 标准控制软件. 本实验中激光能量约为 80 mJ, 能量密度约为 15 J/cm².

2 实验方法

本文天然矿物 Nd 同位素分析的样品制备方法与锆石 U-Pb 年龄与微量元素的样品制备基本相同. 将待测定的天然矿物样品用双面胶粘在载玻片上, 放上 PVC 环, 然后将环氧树脂和固化剂进行充分混合后注入 PVC 环中, 待树脂充分固化后将样品座从载玻片上剥离, 并对其进行抛光, 直到样品露出一个光洁的平面. 样品测定之前用酒精轻擦样品表面后用

稀硝酸超声清洗, 以除去可能的污染.

激光Nd同位素分析与激光测定锆石(斜锆石)Hf同位素分析非常相似 [15], 法拉第杯结构和仪器参数见表 1. 激光剥蚀的斑束直径为 10~120 μm, 频率为 4~10 Hz., 采样方式为单点剥蚀. 以He作为剥蚀物质的载气. 激光剥蚀的物质送入Neptune MC-ICPMS进行Nd同位素测定.

2.1 标准溶液的测定

进行激光Nd同位素测定之前, 我们采用 200 ng·g⁻¹ 的实验室内部标准GSS Nd标准溶液来检验 Neptune MC-ICPMS仪器的稳定性和分析数据的重现性. 长期以来, 实验室内部标准GSS Nd的 ¹⁴³Nd/¹⁴⁴Nd 比值采用 ¹⁴⁶Nd/¹⁴⁴Nd = 0.7219 的指数归一的测定结果平均为 0.511605 ± 0.000024 (2SD, n = 95) (图 1(a)). 对国际标准溶液 La Jolla Nd也进行了跟踪测定, ¹⁴³Nd/¹⁴⁴Nd 比值平均值为 0.511849 ± 0.000014 (2SD, n = 68) (图 1(b)), 与其推荐值 0.511856 ~ 0.511858 [6] 在误差范围内基本一致. 其具体测定过程是先用 3% HNO₃ 进行清洗 2 min, 然后才开始具体样品的测定, 每个样品的总测量时间约为 15 min.

但是, 这一较长的测定方式不适合激光原位 Nd 同位素测定. 为探索适合 Nd 原位测定的方式, 我们在 GSS Nd 的后 26 次测量中未使用 Neptune 的虚拟放大器, 而是采用 0.131 s 的积分时间获得 200 组数据, 总的测量时间约为 30 s. 该情形下单次测量的精度明显低于前面测量的数据, 但 26 次测量获得的

表 1 激光测定 Nd 同位素的法拉第杯结构和仪器参数

法拉第杯结构										
法拉第杯	L4	L3	L2	L1	中心杯	H1	H2	H3	H4	
质量数	142	143	144	145	146	147	149			
待测元素	Nd	Nd	Nd	Nd	Nd					
天然丰度/%	27.13	12.18	23.80	8.30	17.19					
干扰元素	Ce		Sm			Sm	Sm			
天然丰度/%	11.08		3.1			15.0	13.8			
Thermo Finnigan Neptune MC-ICPMS						Lambda Physik Compex UV 193 nm ArF Excimer				
RF 功率: 1304 W						能量密度: ~15 J/cm ²				
冷却气: 15.2 L/min						输出能量: ~80 mJ				
辅助气: 0.8 L/min						束斑直径: 10, 20, 30, 60, 80, 90 和 120 μm				
载气: 0.7 L/min						激光频率: 4, 6, 8 和 10 Hz				
质量分辨率: 400 (Low)						氦气: 0.7~0.8 L/min				
积分时间: 0.131 s										
灵敏度(¹⁴⁶ Nd): 8 V/μg·g ⁻¹										
加速电压: 10 kV										

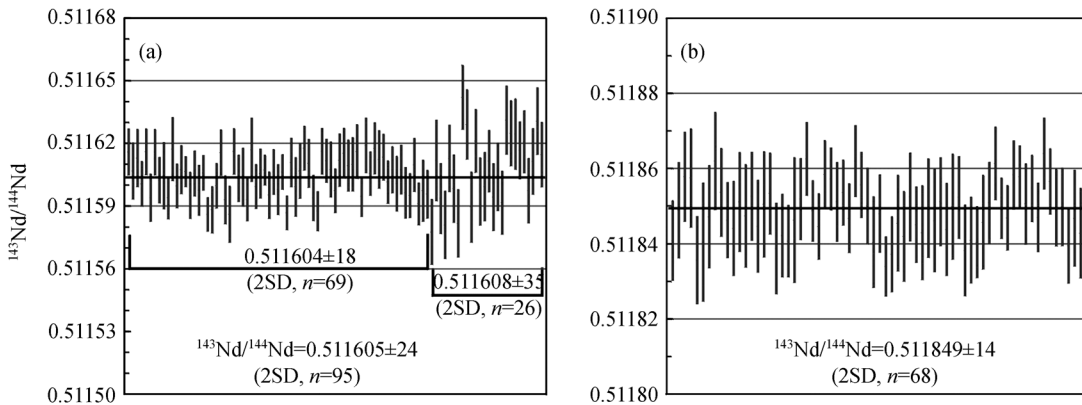


图1 实验室内标准 GSS Nd 和国际标准 La Jolla Nd 测试结果

$^{143}\text{Nd}/^{144}\text{Nd}$ 比值为 0.511608 ± 0.000035 (2SD, $n = 26$) (图 1(a)). 上述实验表明, 两种不同实验方法获得的 Nd 同位素组成极为一致, 即所获得数据的质量基本与积分模式无关. 因此, 我们将在后面的激光原位 Nd 同位素分析中采用 0.131 s 的积分时间. 有关 Neptune MC-ICPMS 测定溶液 Nd 同位素的详细描述参见文献[8].

2.2 同质异位素的干扰校正

激光Nd同位素测定过程中, 由于没有采用任何的分离纯化手段, 必须考虑同质异位素的干扰和基体元素的影响. 对Nd而言, 最主要的干扰来自Ce (^{142}Ce 干扰 ^{142}Nd)和Sm (^{144}Sm 干扰 ^{144}Nd) (表 1). Ce与Nd都属于轻稀土元素, 极为相似地球化学性质, 因此Nd含量高的天然矿物必然含有相当量Ce, 我们以前的工作表明, 大量Ce存在并不影响Nd同位素精确测定, 这就为激光Nd同位素测定具有重要指导意义[8]. 与单聚焦Isoprobe MC-ICPMS不同, 当Ce/Nd比例超过 0.1 时, Ce/Nd与 $^{143}\text{Nd}/^{144}\text{Nd}$ 之间存在线性负相关关系[7]. 至于具体的原因, 目前还不十分清楚, 可能是由于Isoprobe MC-ICPMS采用六极杆(Hexapole)碰撞反应池技术消除能量色散和克服多原子分子离子干扰, 而双聚焦Neptune MC-ICPMS则采用静电分析器来进行能量色散.

Sm的干扰是激光Nd同位素测定中非常关键的问题. 在其他放射成因同位素体系的激光测定过程中, 如Rb-Sr体系, 珊瑚、斜长石、磷灰石、碳酸盐、钙钛矿等低Rb高Sr样品中的Sr同位素可以利用LA-MC-ICPMS测定[16], 再如Lu-Hf体系, LA-MC-

ICPMS测定Hf同位素可以选择低Lu高Hf的样品进行, 如锆石、斜锆石[15]. 但是, 对于Sm-Nd同位素体系而言, 由于Sm与Nd同属于轻稀土元素, 其地球化学性质极其相近, 因而其Sm/Nd比值不存在Rb-Sr或者Lu-Hf体系中出现的情况. 此时, 对干扰的精确扣除成为测试成功与否的关键. 在Nd同位素测定过程中, 最主要的干扰显然来自Sm (表 1), 即 ^{144}Sm 对 ^{144}Nd 的干扰. 一般对它干扰扣除可采用如下方程:

$$[^{144}\text{Nd}]_m = [^{144}(\text{Nd}+\text{Sm})]_m - [^{147}\text{Sm}]_m / [^{147}\text{Sm}/^{144}\text{Sm}]_t \times (M_{147}/M_{144})^{\beta(\text{Sm})}$$

上述公式中, 最关键的是Sm质量分馏(β_{Sm})的确定. 具体方法有 3 种. () 假设Sm与Nd分馏行为完全相同, 该方法对化学分离后残余的少量Sm能够进行有效地扣除[7], 我们以前的实验也表明, 即使Sm/Nd达到 0.04, Neptune MC-ICPMS仍然能够进行有效地进行干扰扣除[8]. 但天然矿物中的Sm/Nd比值一般为 0.1~0.3, 显然不适用该方法来进行激光Nd同位素的干扰校正. () Foster和Vance[11]提出采用迭代方法, 通过反复迭代使得在获得 $^{143}\text{Nd}/^{144}\text{Nd}$ 比值之前, $^{146}\text{Nd}/^{144}\text{Nd}$ 比值趋于一稳定值. 原作者指出, 对于Sm/Nd等于 0.2 样品, 通常需要 4 次迭代, 而对于Sm/Nd高达 1 的样品则需要 10~15 次反复迭代, 显然该方法只是一个经验性结论. () McFarlane和McCulloch[13]提出采用独立无干扰的Sm同位素对 $^{147}\text{Sm}/^{149}\text{Sm} = 1.06119$ 获得Sm的分馏系数, 进而利用 $^{144}\text{Sm}/^{149}\text{Sm} = 0.2103$ 进行 ^{144}Sm 的干扰扣除. 作者也指出, $^{147}\text{Sm}/^{149}\text{Sm} = 1.06119$ 与TIMS值低了约 2%是由于MC-ICPMS较大的分馏行为造成的.

与他们不同的是, 我们采用 $^{147}\text{Sm}/^{149}\text{Sm} =$

1.08680 [17]进行Sm的质量分馏校正, 利用 $^{144}\text{Sm}/^{149}\text{Sm} = 0.22332$ [18]来进行 ^{144}Sm 对 ^{144}Nd 的同质异位素干扰扣除. 该校正方法与LA-MC-ICPMS测定锆石Hf同位素时校正 ^{176}Yb 对 ^{176}Hf 干扰非常相似 [15,19,20]. 图2是激光实际测定过程中Sm与Nd的分馏行为关系, 显然在激光测试过程中, Sm与Nd的分馏是变化的, 且两者不相等. 为考察 ^{144}Sm 对 ^{144}Nd 的干扰是否准确扣除, 我们还可通过稳定的 $^{145}\text{Nd}/^{144}\text{Nd}$ 比值来进行检验 [11,13]. 我们在后文中将会看到, 本文校正后的 $^{145}\text{Nd}/^{144}\text{Nd}$ 比值与其TIMS推荐值 0.348415 [21]在误差范围内基本一致, 从而证明了该校正方法的可行性.

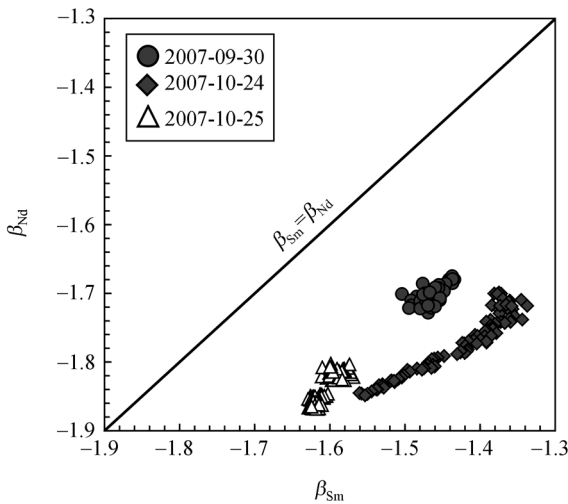


图2 激光测定Nd同位素中Sm与Nd分馏行为关系图

3 激光Nd同位素测定方法

将仪器标定后, 我们便按照上述方法开始进行激光Nd同位素测定. 为研究不同激光参数对测试结果的影响, 我们对一颗来自阿富汗的宝石级磷灰石 (1.5 cm×1 cm×0.5 cm)进行了条件实验. 采用He为载气, 在不同束斑直径(60, 90, 120 μm)、不同工作频率(6, 8, 10 Hz)的原位(*in situ*)激光方式下, 对其Nd同位素组成进行了测定(图3, 表2). 90次测定获得的 $^{143}\text{Nd}/^{144}\text{Nd}$ 比值为 0.511342 ± 31 (2SD), 这与由溶液法获得的 0.511334 ± 10 (2SD, $n = 8$)在误差范围内完全重合. 所获得的 $^{145}\text{Nd}/^{144}\text{Nd}$ 比值为 0.348424 ± 19 (2SD), 与理论值也完全一致, 表明测定方法的正确性.

具体说来, 60 μm时测定的 $^{143}\text{Nd}/^{144}\text{Nd}$ 比值分别为 0.511341 ± 27 (6 Hz), 0.511347 ± 43 (8 Hz)和 0.511346 ± 41 (10 Hz); 90 μm时测定的 $^{143}\text{Nd}/^{144}\text{Nd}$ 比值

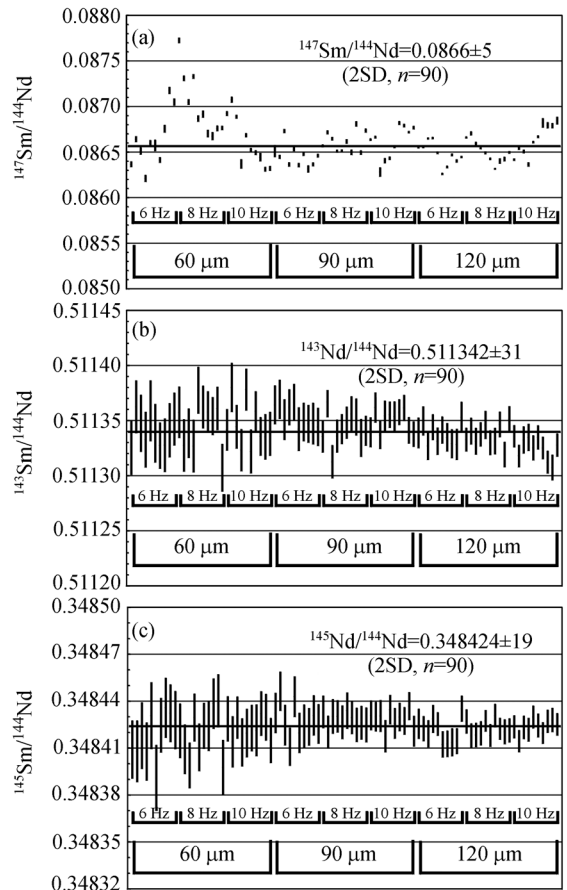


图3 不同激光参数测试磷灰石Nd同位素

为 0.511354 ± 20 (6 Hz), 0.511342 ± 30 (8 Hz)和 0.511350 ± 20 (10 Hz); 而在120 μm时测定的 $^{143}\text{Nd}/^{144}\text{Nd}$ 比值为 0.511338 ± 18 (6 Hz), 0.511337 ± 19 (8 Hz)和 0.511325 ± 20 (10 Hz). 由于信号强度的限制, 我们没有进行30 μm条件下的测定. 实际上, 激光束斑直径的选择取决于样品中Nd的含量, 这在后面的独居石Nd同位素测定中得到充分地说明. 上述3种情形下获得的 $^{143}\text{Nd}/^{144}\text{Nd}$ 比值随束斑直径的增大和激光工作频率的提高, 在误差范围内基本一致, 且随着束斑直径的增大, 所获得的信号强度越高, $^{143}\text{Nd}/^{144}\text{Nd}$ 比值的精度也越来越高(图3), 因此, 在实际应用中, 可以根据实际情况改变激光束斑直径.

4 测定结果

从理论上说, 任何矿物只要具有足够的Nd含量与大小, 均可进行激光Nd同位素测定. 特别是那些富含稀土元素的矿物, 是未来进行激光Nd同位素的重要对象. 但由于这项研究仅处于起步阶段, 目前只

表2 不同激光参数对Nd同位素测试精度的影响(Apatite1)

参数	¹⁴⁶ Nd/V	¹⁴⁷ Sm/V	¹⁴⁷ Sm/ ¹⁴⁴ Nd	¹⁴³ Nd/ ¹⁴⁴ Nd	¹⁴⁵ Nd/ ¹⁴⁴ Nd
60 μm, 6 Hz (n = 10)	1.27	0.15	0.0866±6	0.511341±27	0.348418±29
60 μm, 8 Hz (n = 10)	1.68	0.20	0.0870±7	0.511347±43	0.348419±30
60 μm, 10 Hz (n = 10)	1.86	0.22	0.0866±5	0.511346±41	0.348423±14
90 μm, 6 Hz (n = 10)	2.49	0.30	0.0865±2	0.511354±20	0.348428±21
90 μm, 8 Hz (n = 10)	3.55	0.43	0.0866±2	0.511342±30	0.348428±08
90 μm, 10 Hz (n = 10)	4.37	0.53	0.0866±4	0.511350±20	0.348428±12
120 μm, 6 Hz (n = 10)	5.07	0.61	0.0865±3	0.511338±18	0.348421±16
120 μm, 8 Hz (n = 10)	6.17	0.74	0.0865±2	0.511337±19	0.348422±09
120 μm, 10 Hz (n = 10)	6.95	0.84	0.0866±3	0.511325±20	0.348424±09
平均值(n = 90)	3.71	0.45	0.0866±5	0.511342±31	0.348424±19
溶液测定(n = 8)				0.511334±10	

进行过磷灰石、榍石、铁锰结核、独居石和褐帘石等矿物的有限研究 [11,13]。本文除选择前人尝试过的磷灰石、榍石和独居石做进一步研究外,还对钙钛矿进行了研究。具体测定结果如下(图4)。

磷灰石(Apatite2): 这是另一颗采自阿富汗的宝石,其大小为0.5 cm×1 cm×0.5 cm。在60 μm, 8 Hz和80 μm, 10 Hz两种条件下,我们对该矿物进行的40次测定发现,其¹⁴⁷Sm/¹⁴⁴Nd和¹⁴³Nd/¹⁴⁴Nd均在狭窄的范围内变化,获得的平均值分别为0.0794±13 (2SD)和0.510977±39 (2SD) (图4(a-1)),其¹⁴⁵Nd/¹⁴⁴Nd的平均值为0.348412±17 (2SD) (图4(a-2)),与理论值一致。对该样品运用溶液法获得的8次测定的平均值为0.510985 ± 8 (2SD),与激光测定值在误差范围内一致,这种较低的Nd同位素比值表明其来源于富集源区的结晶。

榍石(O2FW-187): 该样品采自吉林省中部蛟河市境内白石山花岗闪长岩体中的闪长质包体。目前的研究发现 [22],该岩体大约形成于190 Ma左右。包体的野外地质特点和岩石学特征表明它是镁铁质岩浆与寄主岩浆发生混合作用的产物,即与寄主是同时形成的,闪长质包体本身呈黑色,微粒-细粒半自形结构,片麻状构造。主要由斜长石(45%~50%)、黑云母(30%~35%)、角闪石(10%~15%)、和少量石英(5%)与钾长石(<5%)组成。副矿物有磁铁矿、榍石、绿帘石和磷灰石等。其中榍石的粒度大多在0.5~1 mm左右,部分大颗粒可达2 mm。

孙德有等人 [22]曾对该岩体中的两件闪长质包体进行了Sm-Nd同位素测定,获得的¹⁴⁷Sm/¹⁴⁴Nd和¹⁴³Nd/¹⁴⁴Nd比值分别为0.1054、0.1095和0.512626±8和0.512640±14,所对应的ε_{Nd}(t)分别为2.05和2.22。

本文对所采的闪长质包体(O2FW187)中的榍石在60 μm, 10 Hz和120 μm, 8 Hz两种条件下进行了25次测定,结果发现其¹⁴⁷Sm/¹⁴⁴Nd和¹⁴³Nd/¹⁴⁴Nd比值有较大的变化范围,且数据点沿190 Ma的参考等时线分布(图4(b-1))。但¹⁴⁵Nd/¹⁴⁴Nd的平均值为0.348414±34 (2SD)(图4(b-2)),与理论值一致,表明数据本身是可靠的。采用190 Ma的形成年龄,上述25组数据计算的ε_{Nd}(t)平均值为1.7±0.8 (2SD),与由全岩法获得的结果完全一致。

独居石(BY1和BY49): 这是2个采自我国白云鄂博巨型稀土-铌-铁矿区的样品。其中BY1采自都矿区外围都拉哈拉一号火成碳酸岩脉,它侵入于中元古界白云鄂博群H2石英砾岩之中。对该样品中分选的锆石进行测定确定出,该岩脉大约是在14亿年左右形成的,但形成后曾遭到过后期事件的影响 [23]。本文在20 μm, 6 Hz条件下,对该样品中的独居石进行了33次测定,结果发现其¹⁴⁷Sm/¹⁴⁴Nd和¹⁴³Nd/¹⁴⁴Nd比值变化范围较大。去除2个偏离较大的点后,31个数据点获得的等时线年龄为(1.32±0.21) Ga,与锆石U-Pb年龄在误差范围内一致。相应的¹⁴³Nd/¹⁴⁴Nd初始值为0.510885±58(图4(c-1)),ε_{Nd}(t)平均值为0.67 ± 0.94 (2SD),表明该碳酸岩脉来源于近原始地幔的部分熔融。

BY49独居石样品分选自白云鄂博东矿采坑1474 m平台H8白云岩,它是稀土矿化的赋矿围岩。该白云岩样品较纯洁,稀土矿化相对较弱。与BY1不同,BY49样品中的独居石具有较高的¹⁴⁷Sm/¹⁴⁴Nd和¹⁴³Nd/¹⁴⁴Nd比值(图4(c-1))。实验是在10~20 μm, 3~6 Hz的条件下进行的。去除2个高¹⁴⁷Sm/¹⁴⁴Nd比值的样品后,余下38个数据点获得的等时线年龄为(0.86 ± 0.10) Ga,相应的¹⁴³Nd/¹⁴⁴Nd初始值为0.511136±38

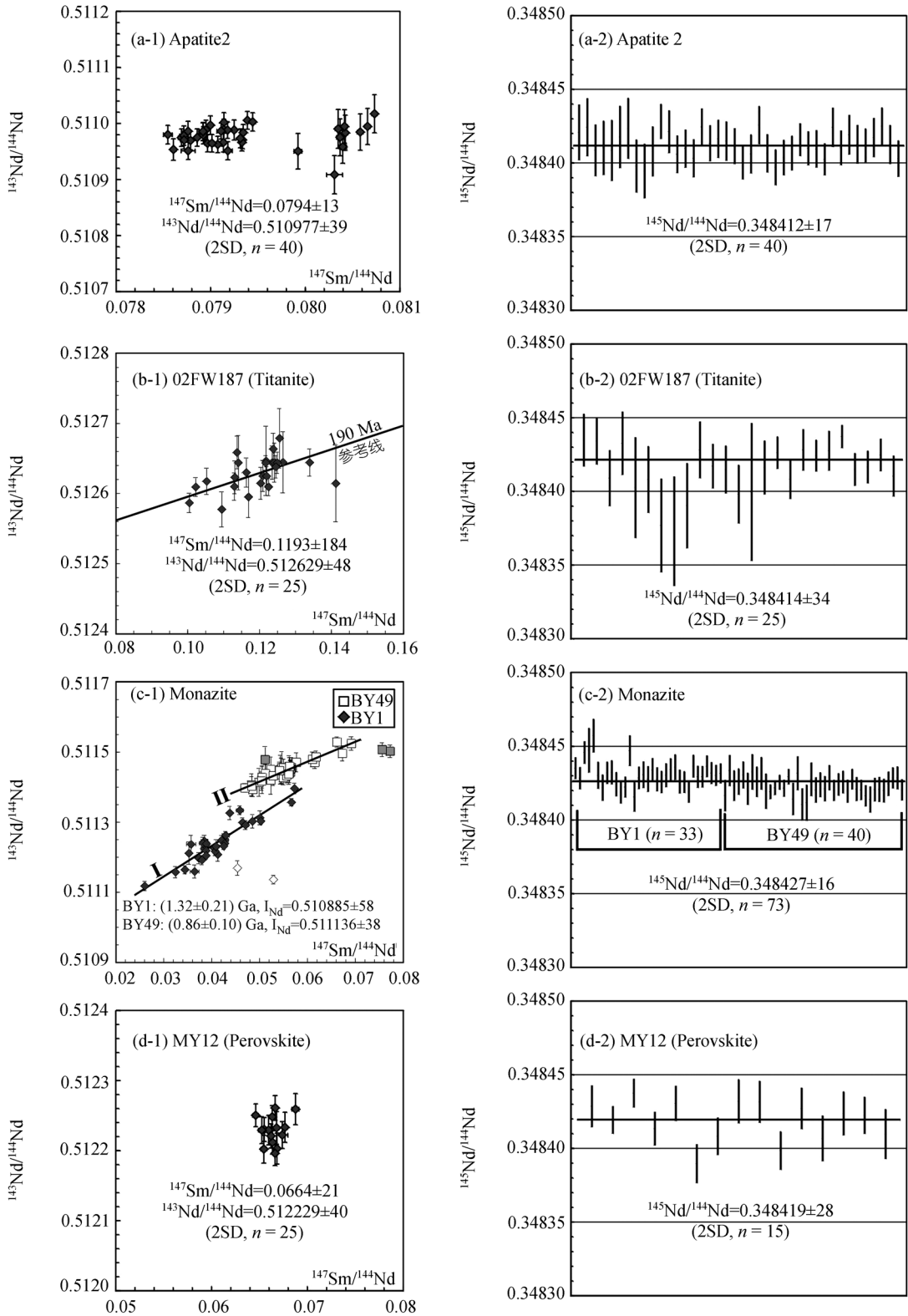


图 4 激光测定磷灰石、榍石、独居石和钙钛矿 Sm-Nd 同位素测试结果

(图4(c-1)). 以 860 Ma 计算的 $\epsilon_{Nd}(t)$ 平均值为 -7.7 ± 0.7 (2SD), 但若以 1400 Ma 计算, 其 $\epsilon_{Nd}(t)$ 平均值为 2.0 ± 0.9 (2SD), 显示源区略亏损的特征.

尽管我们目前还无法对上述 2 个样品的 Nd 同位素差异给出明确的答案, 但本文进行的研究表明, 白云鄂博矿区独居石在 Nd 同位素组成上是不均一的, 特别是稀土矿化寄主白云岩内独居石还可能还遭受过后期 Sm-Nd 同位素体系的扰动, 这可能是导致 Sm-Nd 同位素及独居石 Th-Pb 体系难以对该矿床获得公认形成年龄的重要原因. 由于我们的激光剥蚀直径只有 10~20 μm , 相信今后大量的微区 Nd 同位素研究可能能够揭开这一谜团.

钙钛矿(MY12): 该样品采自山东蒙阴金伯利岩区. 根据以前的研究结果, 这些钙钛矿属于基质矿物, 是金伯利岩岩浆早期结晶的产物 [24]. 在 60 μm , 4 Hz 条件下, 对该矿物进行的 15 次测定发现, 其 $^{147}\text{Sm}/^{144}\text{Nd}$ 和 $^{143}\text{Nd}/^{144}\text{Nd}$ 均在狭窄的范围内变化, 获得的平均值分别为 0.0664 ± 21 (2SD) 和 0.512229 ± 40 (2SD) (图 4(d-1)), 其 $^{145}\text{Nd}/^{144}\text{Nd}$ 的平均值为 0.348419 ± 28 (2SD) (图 4(d-2)), 与理论值一致. 对该样品进行的 2 次溶液法测定获得的 $^{147}\text{Sm}/^{144}\text{Nd}$ 和 $^{143}\text{Nd}/^{144}\text{Nd}$ 比值分别为 0.0686 , 0.0673 和 0.512225 ± 12 (2σ), 0.512235 ± 14 (2σ), 均与激光测定值在误差范围内一致. 按照 470 Ma 的形成年龄, 所计算获得的 $\epsilon_{Nd}(t)$ 平均值为 -0.16 ± 0.78 (2SD), 表明蒙阴金伯利岩来源于近原始的地幔源区.

5 讨论

从以上我们对若干矿物的测定可以看出, 激光 MC-ICPMS 分析可以获得可信的 Nd 同位素数据. 但在实际应用中, 我们需要考虑 2 个问题. 其一是这种方法适用于 Sm/Nd 比值多高的样品; 其二是, 对测定对象的 Nd 含量有何种要求.

对于前者, 我们可以介绍本实验室对 NIST610 玻璃的 Nd 同位素测定情况. 根据多方面的测定, 该玻璃的 Sm, Nd 含量为 441~460 和 429~442 $\mu\text{g/g}$ 左右 [25], 所报道的 2 个 $^{143}\text{Nd}/^{144}\text{Nd}$ 比值分别为 0.511927 ± 4 (2SD, $n = 4$) [26] 和 0.511908 ± 4 (2SD, $n = 3$) [11]. 即该标准的 Sm/Nd 比值约为 1.04, 大约相当于 $^{147}\text{Sm}/^{144}\text{Nd}$ 比值为 0.6277 ± 1 (2SD, $n = 3$) [11]. 我们在 60 μm , 8 Hz 和 80 μm , 10 Hz 条件下, 对该标准玻璃进行了 15 次测定, 所获得的 $^{147}\text{Sm}/^{144}\text{Nd}$ 和 $^{143}\text{Nd}/^{144}\text{Nd}$ 比值分

别为 0.6551 ± 26 (2SD) 和 0.511910 ± 77 (2SD) (图 5), 其 $^{145}\text{Nd}/^{144}\text{Nd}$ 的平均值为 0.348404 ± 74 (2SD). 这一测定表明, 即使对于 Sm/Nd 比值高达 1 的样品而言, 我们仍可获得可信的 $^{143}\text{Nd}/^{144}\text{Nd}$ 比值. 由于受校正的影响, 此时获得的 $^{147}\text{Sm}/^{144}\text{Nd}$ 比值的偏差约在 4% 左右. 考虑自然界中绝大多数样品的 $^{147}\text{Sm}/^{144}\text{Nd}$ 比值集中在 0.1 左右, 我们确信, 激光方法对高 Nd 含量的样品完全可以获得可信的原位 Sm-Nd 同位素数据.

关于激光测定对 Nd 含量的要求, 我们可以用图 6 来加以说明. 将我们前面测定的磷灰石、榍石和钙钛矿的数据进行总结发现, 其信号的强度与测定误差之间呈现一种函数关系(图 6(a)), 根据上述关系确定的不同 Nd 含量样品在不同剥蚀束斑直径下所获得的数据精度如图 6(b) 所示. 样品中 Nd 的含量越高、激光剥蚀束斑直径越大, 或者剥蚀的频率越高, 所获得的信号越强, 所获得的 $^{143}\text{Nd}/^{144}\text{Nd}$ 比值的精度也就越高. 如果假设我们讨论地质问题所要求的误差为 $\pm 2\epsilon$ 单位, 它所对应的 $^{143}\text{Nd}/^{144}\text{Nd}$ 比值误差约为 0.0001. 在 60 μm 和 8 Hz 情形下, 所要求的样品的最低 Nd 含量约为 200 $\mu\text{g/g}$. 但我们相信, 随着技术的发展, 未来激光测定对 Nd 含量的要求还会有所降低. 因此, 虽然通常的地质样品不能用激光方法来获得可信的 Nd 同位素数据, 但像磷灰石、榍石、褐帘石、磷钇矿、萤石、独居石和钙钛矿等富含稀土元素的矿物, 目前的技术完全可以获得所要求的数据. 特别是对于前面所测定的富含稀土元素的独居石而言, 在 8 Hz 的条件下, 5~10 μm 的束斑直径便可获得足够的精度数据. 由于上述矿物在自然界中广泛存在, 且是同位素定年研究的重要对象 [27], 因此激光 Nd 同位

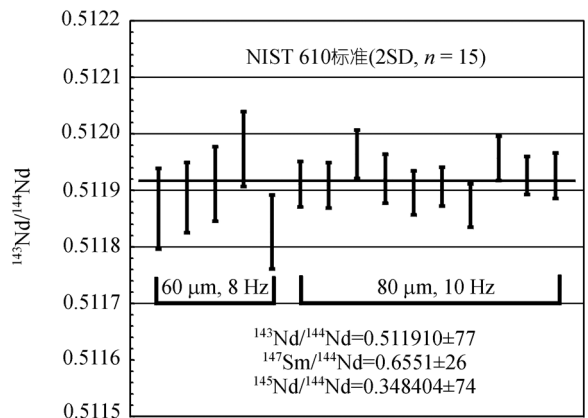


图 5 NIST 610 标准玻璃的激光 Nd 同位素测定结果

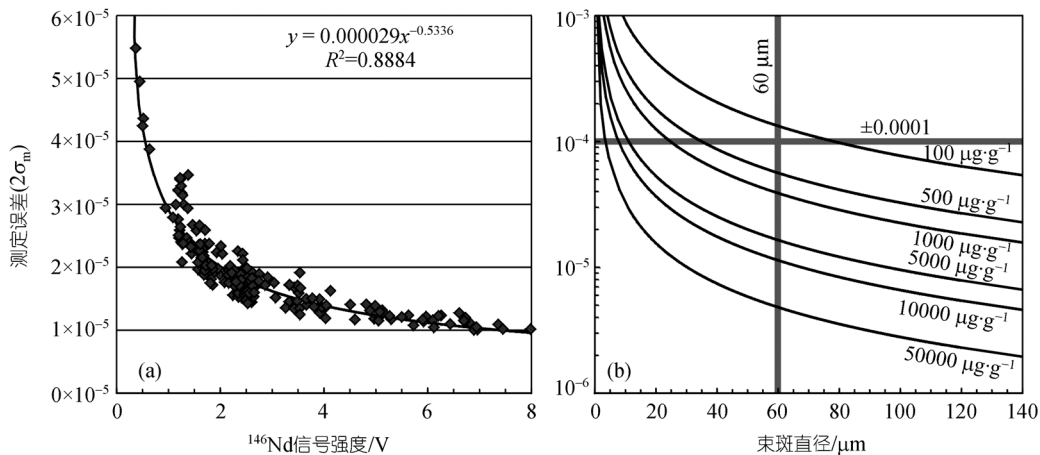


图6 激光剥蚀条件下地质样品Nd含量与测定精度的关系

素测定将会在未来的固体地球科学研究中发挥非常重要的作用。

6 结论

() 采用 Neptune MC-ICPMS 和 Geolas 193 nm ArF 准分子激光剥蚀系统进行 Nd 同位素的激光测定发现, Sm 和 Nd 的质量歧视行为在激光剥蚀情形下是不同的, 并具有随时间变化的特征。

() 对高 Nd 含量的地质样品而言, 采用新发表

的 Sm 同位素丰度比值可以对同质异位素的干扰进行准确扣除, 从而可以对磷灰石、榍石、独居石和钙钛矿等天然矿物的 $^{143}\text{Nd}/^{144}\text{Nd}$ 和 $^{147}\text{Sm}/^{144}\text{Nd}$ 比值进行精确的测定。

() 激光剥蚀过程中束斑直径大小的选择取决于样品的 Nd 含量。对于像独居石这样富集稀土元素的矿物, 5 μm 情形下即可获得可信的 Nd 同位素数据, 从而为矿物微区 Nd 同位素研究提供了重要技术手段。

致谢 丘志力教授提供阿富汗磷灰石样品。两位匿名审稿人审阅了论文, 并提出了具体的修改意见。在此一并致以诚挚的谢意。

参考文献

- 1 Faure G, Mensing T M. *Isotopes: Principles and Applications*. 3rd ed. New Jersey: John Wiley & Sons, 2005. 75—112, 436—451
- 2 Chen F K, Hegner E, Todt W. Zircon ages, Nd isotopic and chemical compositions of orthogneisses from the Black Forest, Germany—evidence for a Cambrian magmatic arc. *Int J Earth Sci*, 2000, 88: 791—802 [\[DOI\]](#)
- 3 Halliday A N, Lee D C, Christensen J N, et al. Recent developments in inductively coupled plasma magnetic sector multiple collector mass spectrometry. *Int J Mass Spectrom Ion Proc*, 1995, 146-147: 21—33 [\[DOI\]](#)
- 4 Halliday A N, Lee D C, Christensen J N, et al. Applications of multiple collector-ICPMS to cosmochemistry, geochemistry, and paleoceanography. *Geochim Cosmochim Acta*, 1998, 62: 919—940 [\[DOI\]](#)
- 5 Luais B, Telouk P, Albaredo F. Precise and accurate neodymium isotopic measurements by plasma-source mass spectrometry. *Geochim Cosmochim Acta*, 1997, 61: 4847—4854 [\[DOI\]](#)
- 6 Vance D, Thirlwall M. An assessment of mass discrimination in MC-ICPMS using Nd isotopes. *Chem Geol*, 2002, 185: 227—240 [\[DOI\]](#)
- 7 梁细荣, 韦刚健, 李献华, 等. 利用 MC-ICPMS 精确测定 $^{143}\text{Nd}/^{144}\text{Nd}$ 和 Sm/Nd 比值. *地球化学*, 2003, 32(1): 91—95
- 8 杨岳衡, 张宏福, 谢烈文, 等. 多接收器电感耦合等离子体质谱精确测定钆同位素组成. *分析化学*, 2007, 35(1): 71—74
- 9 何学贤, 唐索寒, 朱祥坤, 等. 多接收器等离子体质谱(MC-ICPMS)高精度测定 Nd 同位素方法. *地球学报*, 2007, 28: 405—410

- 10 Rehkamper M, Schonbachler M, Stirling C H. Multiple collector ICP-MS: Introduction to instrumentation, measurement techniques and analytical capabilities. *Geostand Newsl*, 2001, 25: 23—40 [\[DOI\]](#)
- 11 Foster G L, Vance D. *In situ* Nd isotopic analysis of geological materials by laser ablation MC-ICP-MS. *J Anal Atomic Spectro*, 2006, 21: 288—296 [\[DOI\]](#)
- 12 Foster G L, Carter A. Insights into the patterns and locations of erosion in the Himalaya—A combined fission-track and *in situ* Sm-Nd isotopic study of detrital apatite. *Earth Planet Sci Lett*, 2007, 257: 407—418 [\[DOI\]](#)
- 13 McFarlane C R M, McCulloch M T. Coupling of *in-situ* Sm-Nd systematics and U-Pb dating of monazite and allanite with applications to crustal evolution studies. *Chem Geol*, 2007, 245: 45—60 [\[DOI\]](#)
- 14 徐平, 吴福元, 谢烈文, 等. O-Pb 同位素定年标准锆石的 Hf 同位素. *科学通报*, 2004, 49(14): 1403—1410
- 15 Wu F Y, Yang Y H, Xie L W, et al. Hf isotopic compositions of the standard zircons and baddeleyites used in U-Pb geochronology. *Chem Geol*, 2006, 234: 105—126 [\[DOI\]](#)
- 16 Ramos F C, Wolff J A, Tollstrup D L. Measuring $^{87}\text{Sr}/^{86}\text{Sr}$ variation in minerals and groundmass from basalts using LA- MC-ICPMS. *Chem Geol*, 2004, 211: 135—158 [\[DOI\]](#)
- 17 Dubois J C, Retali G, Cesario J. Isotopic analysis of rare earth elements by total vaporization of samples in thermal ionization mass spectrometry. *Int J Mass Spectrom Ion Process*, 1992, 120: 163—177 [\[DOI\]](#)
- 18 Isnard H, Brennetot R, Caussignac C, et al. Investigations for determination of Gd and Sm isotopic compositions in spent nuclear fuels samples by MC ICPMS. *Int J Mass Spectro*, 2005, 246: 66—73 [\[DOI\]](#)
- 19 Woodhead J, Hergt J, Shelley M, et al. Zircon Hf-isotope analysis with an excimer laser, depth profiling, ablation of complex geometries, and concomitant age estimation. *Chem Geol*, 2004, 209: 121—135 [\[DOI\]](#)
- 20 Yuan H L, Gao S, Dai M N, et al. Simultaneous determinations of U-Pb age, Hf isotopes and trace element compositions of zircon by excimer laser ablation quadrupole and multiple collector ICP-MS. *Chem Geol*, 2008, 247: 100—118
- 21 Wasserburg G J, Jacobsen S B, DePaolo D J, et al. Precise determination of Sm/Nd ratios, Sm and Nd isotopic abundances in standard solutions. *Geochim Cosmochim Acta*, 1981, 45: 2311—2323 [\[DOI\]](#)
- 22 孙德有, 吴福元, 林强, 等, 张广才岭燕山早期白石山岩体成因与壳幔相互作用. *岩石学报*, 2001, 17: 227—235
- 23 范宏瑞, 胡芳芳, 陈福坤, 等. 白云鄂博超大型 REE-Nb-Fe 矿区碳酸岩墙的侵位年龄——兼答 Le Bas 博士的质疑. *岩石学报*, 2006, 22: 519—520
- 24 池际尚, 路凤香. 华北地台金伯利岩及古生代岩石圈地幔特征. 北京: 科学出版社, 1996
- 25 Rocholl A, Dulski P, Raczek I. New ID-TIMS, ICP-MS and SIMS data on the trace element composition and homogeneity of NIST certified reference material SRM 610-611. *Geostand Newsl*, 2000, 24: 261—274 [\[DOI\]](#)
- 26 Woodhead J D, Hergt J M. Strontium, Neodymium and Lead isotope analyses of NIST glass certified reference materials: SRM 610, 612, 614. *Geostand Newsl*, 2001, 25(2-3): 261—266 [\[DOI\]](#)
- 27 Poitrasson F, Hancher J M, Schaltegger U. The current state and future of accessory mineral research. *Chem Geol*, 2002, 191: 3—24 [\[DOI\]](#)

In situ Nd isotopic measurement of natural geological materials by LA-MC-ICPMS

YANG YueHeng, SUN JinFeng, XIE LieWen, FAN HongRui & WU FuYuan[†]

State Key Laboratory of Lithospheric Evolution, Institute of Geology and Geophysics, Chinese Academy of Sciences, Beijing 100029, China

Using newly determined Sm isotopic abundances for correcting the isobaric interference of ^{144}Sm on ^{144}Nd and the established mass bias relationship between Sm and Nd, a series of *in situ* Nd isotopic measurements were conducted for relatively high Nd concentrations of natural geological materials, including apatite, titanite, monazite and perovskite on a Neptune multi-collector inductively coupled plasma mass spectrometry (MC-ICPMS), coupled to a 193 nm ArF excimer laser ablation system. The results show that Ce has no significant influence on the precision and accuracy of Nd isotopic analyses for LREE-enriched geological minerals and that our approach is efficient in obtaining reliable $^{143}\text{Nd}/^{144}\text{Nd}$ and $^{147}\text{Sm}/^{144}\text{Nd}$ ratios for those materials with $\text{Sm}/\text{Nd} < 1$ ($^{147}\text{Sm}/^{144}\text{Nd} < 0.6$). When combined with trace element and U-Pb isotope data, the *in situ* Nd isotopic data can provide important information on geological processes.

Nd isotope, apatite, titanite, monazite, perovskite, LA-MC-ICPMS

Nd isotopes are not only an important tracer in geochemistry and geochronology, but also one of the most important tools for deciphering petrogenesis and crust-mantle evolution of the Earth^[1]. Traditionally, Nd isotopic data can be obtained by chemical separation of Sm and Nd using at least two ion-exchange columns after complete sample digestion, followed by purification of the Nd fraction, and then isotopic measurement by Thermal Ionization Mass Spectrometry (TIMS)^[2]. However, there have been two significant developments in isotopic geochemistry in recent years. Firstly, MC-ICPMS has been widely used for numerous isotopic measurements^[3,4]. In terms of Nd isotope, the MC-ICPMS solution technique can obtain reliable Nd isotopic data, comparable to the TIMS method^[5–9]. However, the solution method is a bulk analysis and the Nd isotope data are therefore average of the sample. Since most natural minerals have some compositional zonation, obtaining isotopic variation within individual mineral grains has become another important development and frontier in isotopic geochemistry. For example, ion and laser probe

techniques have been widely applied for *in situ* isotope measurement. Since the ion source of the MC-ICPMS is under atmospheric pressure, it makes easier and more convenient to change the sampling mode. Equipped with a laser ablation (LA) system, *in-situ* isotope measurements can be easily conducted. The LA-MC-ICPMS technique has distinct advantages over traditional bulk analysis in that it can decipher subtle isotopic variations at high spatial resolution on a sub-grain scale and does not need time-consuming sample preparation; it is therefore high efficient. Currently, the LA-MC-ICPMS technique has been widely used in Sr, Hf, Os, B and Mg isotopic measurements^[10] and provided a great deal of important constraints on the geological processes. Comparatively, there are few studies of *in situ* Nd isotopic analyses due to the isobaric interference of Sm on Nd during laser ablation analysis. Nevertheless, some

Received November 23, 2007; accepted January 14, 2008

doi: 10.1007/s11434-008-0166-z

[†]Corresponding author (email: wufuyuan@mail.igcas.ac.cn)

Supported by the National Natural Science Foundation of China (Grant Nos. 40773008 and 40325006)

researchers have done pioneering work^[11–13], and provided reliable data for apatite, titanite, ferromanganese nodules, monazite and allanite, indicating its potential applications in geology. In this paper, a series of *in situ* Nd isotopic measurements have been carried out on a Neptune MC-ICPMS machine coupled with 193 nm ArF excimer laser system for minerals with a relatively high Nd concentration, including apatite, titanite, monazite and perovskite.

1 Instrumentation

Nd isotope measurements were carried out on a Thermo-Finnigan Neptune MC-ICPMS, coupled with a 193 nm ArF Excimer laser ablation system, at the State Key Laboratory of Lithospheric Evolution in the Institute of Geology and Geophysics, Chinese Academy of Sciences in Beijing, China. The details of this machine can be inferred to refs. [14, 15].

The GeoLas Plus 193 nm Excimer ArF laser ablation system is the upgrade product of GeoLas CQ made by Lambda Physik in Germany. It consists of the following three parts: (1) a COMpex 102 ArF Excimer laser generator with wavelength of 193 nm, maximum energy of 200 mJ, pulse width of 15 ns and frequency from 1 to 20 Hz; (2) a laser optical system with a laser beam homogenizing system, consisting of two 13×13 lens arrays. The laser spot size can be adjusted to 4, 10, 20, 30, 40, 50, 60, 70, 80, 90, 100, 110, 120, 130, 160 μm; and (3) Geolas standard software. The highest energy density is 35 J/cm², but only 15 J/cm² was used in this study.

2 Analytical procedures

The sample preparation for *in situ* Nd isotope measurement in this work is almost the same as that of zircon U-Pb and trace element analysis by LA-ICP-MS. Naturally separated minerals were placed onto a piece of glass with double-sided tape under a binocular microscope and a PVC ring was then placed on it. Then, a mixture of epoxy and hardener was put into the PVC ring and allowed to totally solidify. Finally, the mount was peeled off from the glass and polished until the surface became even and the sample was revealed. Before analysis, the sample surface was cleaned ultrasonically with ethanol and trace HNO₃ to eliminate possible contamination.

The laser ablation Nd isotope analysis is almost the same as that of zircon Hf isotope analysis^[15], with experimental conditions and cup configurations for Nd isotopic analyses are shown in Table 1. The laser spot size can be changed from 10–120 μm at 10 μm interval and 4–10 Hz of pulse rate. The aerosol ablated by the laser was transported to the mass spectrometer using helium as the carrier gas.

2.1 Standard solution analysis

Our in-house standard solution GSS Nd with 200 ppb of Nd was used for evaluating the reproducibility and accuracy of the Neptune MC-ICPMS for Nd isotope measurement prior to laser ablation analysis. The average ¹⁴³Nd/¹⁴⁴Nd ratios for the GSS Nd standard solution over two years is 0.511605±0.000024 (2SD, *n* = 95) (Figure 1(a)), normalized to ¹⁴⁶Nd/¹⁴⁴Nd = 0.7219 using

Table 1 Faraday cup configuration and instrument operating parameters

Faraday cup configuration									
Cups	L4	L3	L2	L1	Center	H1	H2	H3	H4
Nominal mass	142	143	144	145	146	147	149		
Measured elements	Nd	Nd	Nd	Nd	Nd				
Natural abundance (%)	27.13	12.18	23.80	8.30	17.19				
Interfering elements	Ce		Sm			Sm	Sm		
Natural abundance in (%)	11.08		3.1			15.0	13.8		
Instrument parameters									
Thermo Finnigan Neptune MC-ICPMS					Lambda Physik Compex UV 193 nm ArF Excimer				
RF forward power	1304 W					Fluence	~15 J/cm ²		
Cooling gas	15.2 L/min					Output power	~80 mJ		
Auxiliary gas	0.8 L/min					Spot size	10, 20, 30, 60, 80, 90 and 120 μm		
Sample gas	0.7 L/min					Pulse rate	4, 6, 8 and 10 Hz		
Mass resolution	400 (Low)					He gas to cell	0.7 to 0.8 L/min		
Integration time	0.131 s								
Sensitivity on ¹⁴⁶ Nd	8 V/ppm								
Acceleration voltage	10 kV								

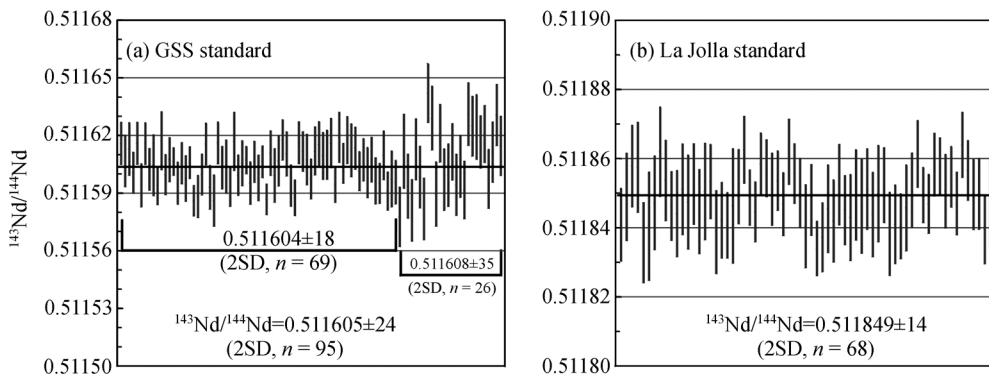


Figure 1 Nd isotopic measurement for in-house GSS Nd and La Jolla Nd standards.

the exponential law for mass bias correction. At the same time, the average of $^{143}\text{Nd}/^{144}\text{Nd}$ for the international La Jolla Nd standard solution is 0.511849 ± 0.000014 (2SD, $n = 68$) (Figure 1(b)), which is identical, within error, to the recommended values of 0.511856–0.511858 by MC-ICPMS^[6]. The standard introduction system was washed with 3% HNO_3 for two minutes prior to actual sample measurement, and it takes totally about 15 minutes for one sample measurement.

Laser ablation signal endurance is much shorter than that of solution analysis, so alternative method was carried out of one block with 200 cycles, in which one cycle has 0.131 second integration time and a total time for one measurement lasts about 30 seconds. Using this sampling model, the average $^{143}\text{Nd}/^{144}\text{Nd}$ for the GSS Nd standard solution is 0.511608 ± 0.000035 (2SD, $n = 26$) (Figure 1(a)), which is exactly the same as the first 69 measurements obtained by the method mentioned above, although the precision of the individual analyses was about two orders of magnitude lower. These results indicate that equivalent isotopic data can be obtained by different sampling methods. We, therefore, use this model in laser ablation analysis. The details of the Nd isotopic analyses can be found elsewhere^[8].

2.2 Isobaric interference correction

As in all laser ablation methodologies great care must be taken to avoid or mitigate the effects of isobaric interferences. *In situ* Nd isotopes the problem interferences are principally caused by Ce (^{142}Ce on ^{142}Nd) and Sm (^{144}Sm on ^{144}Nd) (Table 1). Since both Ce and Nd show almost identical geochemical characters as light rare earth elements (LREE) in the periodic table, the higher Nd concentration, the higher Ce concentration in natural geological materials. Our previous work indicated that

the influence of Ce on Nd isotope analysis is insignificant even Ce/Nd ratio up to 3, which is normal value in the natural geological materials. This conclusion has significant implications for *in situ* Nd measurement by LA-MC-ICPMS^[8]. Absolutely different from Isoprobe MC-ICPMS, there will be negative relationship between Ce/Nd ratio and $^{143}\text{Nd}/^{144}\text{Nd}$ when Ce/Nd ratio more than 0.1^[7]. Although the concrete reason is still unknown at present, it is Hexapole collision cell for different ion dynamic energy dispersion and polyatomic interference while electronic static analysis (ESA) adopted by Neptune.

During measurements of other radiogenic isotopes, samples with low concentration of the parent element, and subsequently low parent/daughter ratios were selected, such as coral, plagioclase, apatite, carbonate and perovskite for the Rb-Sr system^[16], and zircon and baddeleyite for the Lu-Hf system^[15]. Unlike Rb-Sr or Lu-Hf isotopic systems, however, there is no mineral having low Sm/Nd ratio like those in the Rb-Sr and Lu-Hf systems since both Sm and Nd show almost identical geochemical characters as light rare earth elements (LREE) in the periodic table. Therefore the most crucial thing during *in situ* Nd isotope measurement is how to process precisely the isobaric interference of ^{144}Sm on ^{144}Nd . Generally, the subtraction equation of isobaric interference of ^{144}Sm on ^{144}Nd can be expressed as:

$$[^{144}\text{Nd}]_m = [^{144}(\text{Nd} + \text{Sm})]_m - [^{147}\text{Sm}]_m / [^{147}\text{Sm}/^{144}\text{Sm}]_t \times (M_{147}/M_{144})^{\beta(\text{Sm})}$$

The key point during actual analyses is determination of the mass bias of Sm in the above equation, which can be obtained by three approaches: (1) The first is assuming that both Sm and Nd have identical mass biases, which would be very feasible for isobaric interference

correction when only small Sm existed in the Nd fraction after chemical separation^[7]. It was evident in our previous work that the Neptune MC-ICPMS can make accurate isobaric correction even if the Sm/Nd ratio is up to 0.04 in the Nd fraction^[8]. Obviously, this isobaric correction approach is unfeasible for laser ablation analysis because the Sm/Nd ratio is in the range of 0.1–0.3 for most natural minerals. (2) Foster and Vance^[11] advocated an iterative approach for the Sm correction, in which the $^{146}\text{Nd}/^{144}\text{Nd}$ ratio will converge to a stable value after several iterations for various Sm/Nd ratios prior to normalizing the $^{143}\text{Nd}/^{144}\text{Nd}$ ratio using the exponential law. Moreover, they also pointed out that four iterations were needed for a Sm/Nd ratio of around 0.2, while 10–15 iterations are required for a Sm/Nd ratio as high as 1. Obviously, this approach is an empirical and irrational conclusion. (3) McFarlane and McCulloch^[13] proposed that the β_{Sm} value can be directly obtained from the $^{147}\text{Sm}/^{149}\text{Sm}$ ratio on the sample itself and then applied in the isobaric interference correction of ^{144}Sm on ^{144}Nd . They also pointed out that these values are ~2% lower than TIMS values owing to the larger mass bias inherent to plasma-source mass spectrometers.

Unlike the recommended value, the newly obtained $^{147}\text{Sm}/^{149}\text{Sm}$ ratio of 1.08680^[17] and $^{144}\text{Sm}/^{149}\text{Sm}$ ratio of 0.22332^[18] determined by MC-ICPMS are used for the isobaric correction of ^{144}Sm on ^{144}Nd in this study. This approach is almost the same as that of ^{176}Yb on ^{176}Hf during *in situ* zircon Lu-Hf isotopic analysis^[15,19,20]. Our experiments indicated that mass bias of Sm and Nd (β_{Sm} and β_{Nd}) was not equal, changing with analytical emission (Figure 2). In addition, the stable $^{145}\text{Nd}/^{144}\text{Nd}$ ratio

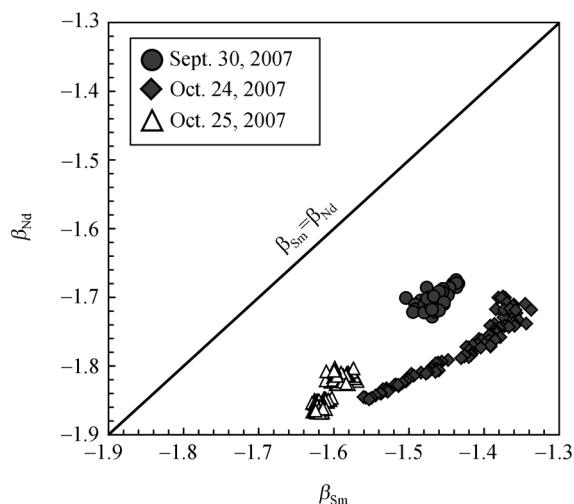


Figure 2 Variations of mass bias between Sm and Nd during laser ablation analyses.

can be also used to evaluate the feasibility of our method^[11,13]. It will be shown below that our normalized $^{145}\text{Nd}/^{144}\text{Nd}$ ratios after isobaric interference correction agree well with the recommended value, within error, of 0.348415 obtained by TIMS^[21].

3 Analytical protocols for *in situ* Nd isotope

After calibration, the Nd isotope measurements were subsequently conducted. In order to evaluate measurements under different laser parameters, an apatite gem (1.5 cm×1 cm×0.5 cm) from Afghanistan was analyzed. *In situ* laser ablation analyses were carried out with spot sizes of 60, 90 and 120 μm with repetition pulse rates of 6, 8 and 10 Hz. Under each condition, 10 measurements were conducted and the average $^{147}\text{Sm}/^{144}\text{Nd}$, $^{143}\text{Nd}/^{144}\text{Nd}$ and $^{145}\text{Nd}/^{144}\text{Nd}$ ratios, with 2SD, were obtained (Figure 3; Table 2). The average $^{143}\text{Nd}/^{144}\text{Nd}$ ratio of 90 measurements was 0.511342 \pm 31 (2SD), which agrees well with that of 0.511334 \pm 10 (2SD, $n=8$) ob-

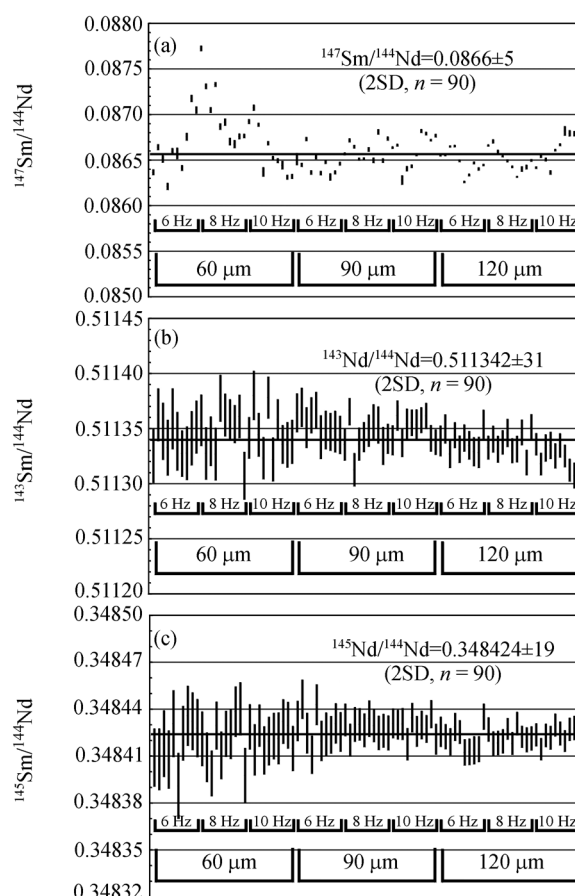


Figure 3 Nd isotope analyses of apatite using different spot sizes and pulse rates.

Table 2 Nd isotopic analyses using different laser parameters (Apatite1)

Parameters	^{146}Nd (V)	^{147}Sm (V)	$^{147}\text{Sm}/^{144}\text{Nd}$	$^{143}\text{Nd}/^{144}\text{Nd}$	$^{145}\text{Nd}/^{144}\text{Nd}$
60 μm , 6 Hz ($n=10$)	1.27	0.15	0.0866 \pm 6	0.511341 \pm 27	0.348418 \pm 29
60 μm , 8 Hz ($n=10$)	1.68	0.20	0.0870 \pm 7	0.511347 \pm 43	0.348419 \pm 30
60 μm , 10 Hz ($n=10$)	1.86	0.22	0.0866 \pm 5	0.511346 \pm 41	0.348423 \pm 14
90 μm , 6 Hz ($n=10$)	2.49	0.30	0.0865 \pm 2	0.511354 \pm 20	0.348428 \pm 21
90 μm , 8 Hz ($n=10$)	3.55	0.43	0.0866 \pm 2	0.511342 \pm 30	0.348428 \pm 08
90 μm , 10 Hz ($n=10$)	4.37	0.53	0.0866 \pm 4	0.511350 \pm 20	0.348428 \pm 12
120 μm , 6 Hz ($n=10$)	5.07	0.61	0.0865 \pm 3	0.511338 \pm 18	0.348421 \pm 16
120 μm , 8 Hz ($n=10$)	6.17	0.74	0.0865 \pm 2	0.511337 \pm 19	0.348422 \pm 09
120 μm , 10 Hz ($n=10$)	6.95	0.84	0.0866 \pm 3	0.511325 \pm 20	0.348424 \pm 09
Summary ($n=90$)	3.71	0.45	0.0866 \pm 5	0.511342 \pm 31	0.348424 \pm 19
Solution analyses ($n=8$)				0.511334 \pm 10	

tained by purified solution MC-ICPMS analyses. In addition, the average $^{145}\text{Nd}/^{144}\text{Nd}$ ratio of 90 measurements was 0.348424 ± 19 (2SD), identical to the recommended value.

Specifically, the average $^{143}\text{Nd}/^{144}\text{Nd}$ ratio under 60 μm spot size was 0.511341 ± 27 (6 Hz), 0.511347 ± 43 (8 Hz) and 0.511346 ± 41 (10 Hz), respectively. The average $^{145}\text{Nd}/^{144}\text{Nd}$ ratio under 90 μm was 0.511354 ± 20 (6 Hz), 0.511342 ± 30 (8 Hz) and 0.511350 ± 20 (10 Hz), respectively. Under 120 μm spot size, the average $^{143}\text{Nd}/^{144}\text{Nd}$ ratio was 0.511338 ± 18 (6 Hz), 0.511337 ± 19 (8 Hz) and 0.511325 ± 20 (10 Hz), respectively. The measurement under 30 μm spot size was not carried out due to signal intensity limitation. Actually, selection of laser spot size was dependent on the Nd concentration of sample, which will be illuminated in detail for monazite measurements below. Whatever, the obtained $^{143}\text{Nd}/^{144}\text{Nd}$ ratios for 3 different spot sizes are identical within errors and the signal intensity increases with increasing of spot size. A higher precision is obtained when a larger spot size is ablated (Figure 3).

4 Results

Theoretically speaking, *in situ* Nd isotope measurement can be conducted on any minerals with enough Nd concentration and size. Especially, the REE-enriched minerals will be important and prospective objects for laser ablation Nd isotope analysis. However, this kind of work is still in its pioneering stage and only a few researches of *in situ* measurements are conducted on apatite, titanite, ferromanganese nodules, monazite and allanite^[11,13]. In this study, not only apatite, titanite and monazite were further studied, but also perovskite was first performed for *in situ* Nd isotope measurement. The results are described as follows (Figure 4).

Apatite2. This is another gem from Afghanistan (0.5 cm \times 1 cm \times 0.5 cm). The average $^{147}\text{Sm}/^{144}\text{Nd}$ and $^{143}\text{Nd}/^{144}\text{Nd}$ ratios of 40 measurements with spot sizes of 60 μm (8 Hz) and 80 μm (10 Hz) were 0.0794 ± 13 (2SD) and 0.510977 ± 39 (2SD) (Figure 4(a-1)), respectively, indicating its narrow variation. Additionally, the average $^{145}\text{Nd}/^{144}\text{Nd}$ ratio was 0.348412 ± 17 (2SD) (Figure 4(a-2)), agreeing well with the recommended value. The average $^{143}\text{Nd}/^{144}\text{Nd}$ ratio of 8 measurements by purified solution using the MC-ICPMS method was 0.510985 ± 8 (2SD), which was identical to that obtained by laser ablation analyses. The lower Nd isotopic ratio indicates its derivation from an isotopically enriched source.

Titanite (02FW-187). This sample was collected from a dioritic enclave in the Baishishan granodiorite in Jiaohe, Jilin Province. It is considered that the Baishishan pluton was emplaced at ~ 190 Ma^[22]. Field and petrographic investigations indicate that the enclave is the product of magma mixing of mafic magma with host granitic magmas, i.e., both the granite and enclave are coeval. The dioritic enclave is black with fine-grained texture and gneissic structure. The minerals include plagioclase (45%–50%), biotite (30%–35%), hornblende (10%–15%), quartz ($\leq 5\%$) and K-feldspar ($< 5\%$), with accessory magnetite, titanite, epidote and apatite. Most titanites have a grain size of 0.5–1 mm, with a maximum of 2 mm.

Sun et al.^[22] conducted Sm-Nd isotopic analyses on 2 samples of the enclave and got $^{147}\text{Sm}/^{144}\text{Nd}$ and $^{143}\text{Nd}/^{144}\text{Nd}$ ratios of 0.1054, 0.1095, and 0.512626 ± 8 and 0.512640 ± 14 , corresponding to $\epsilon_{\text{Nd}}(t)$ values of 2.05 and 2.22. Twenty-five analyses of titanite from diorite enclave (02FW187) using both 60 μm and 10Hz, and 120 μm and 8 Hz suggested that there are some variations in the $^{147}\text{Sm}/^{144}\text{Nd}$ and $^{143}\text{Nd}/^{144}\text{Nd}$ ratios, but all

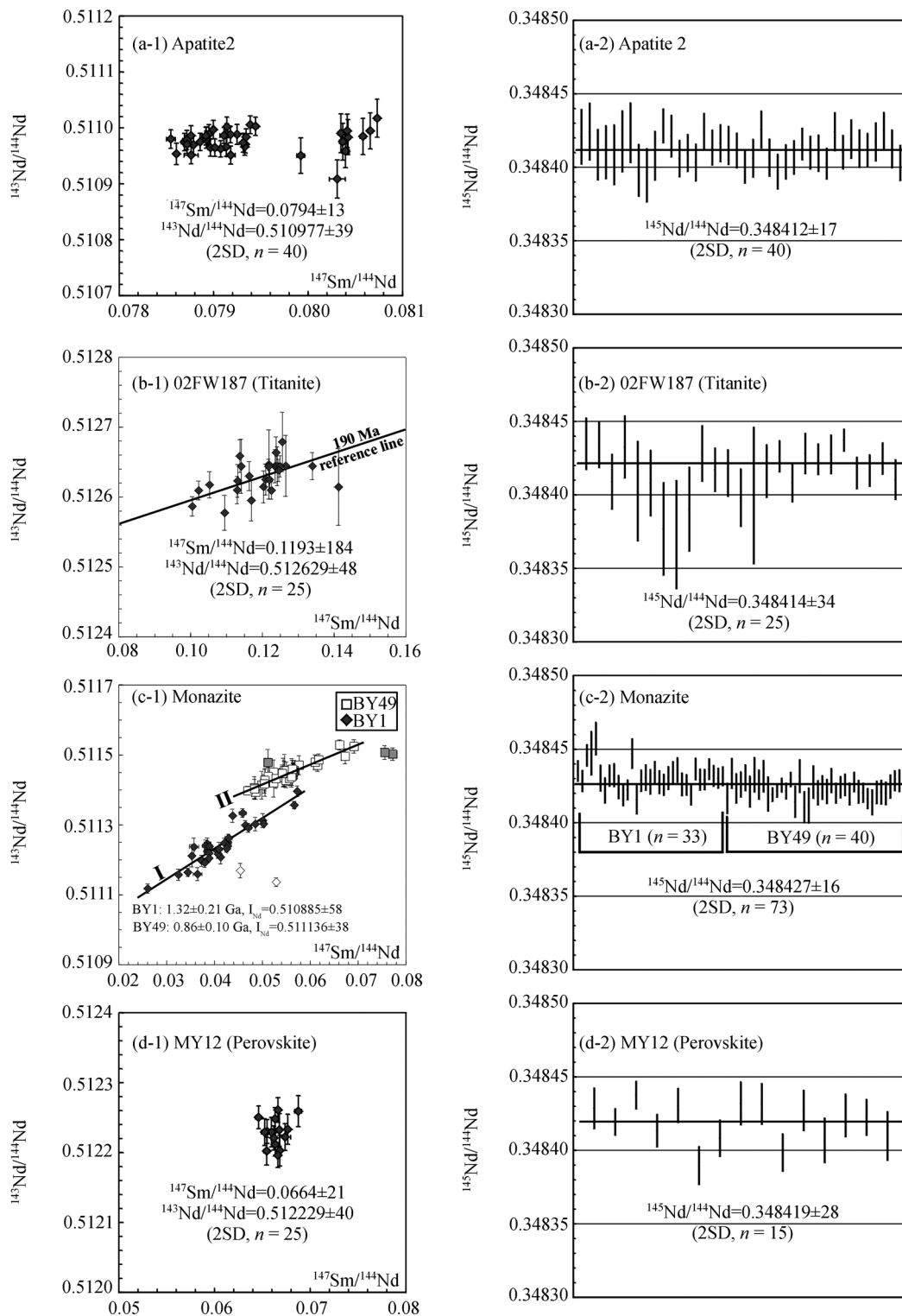


Figure 4 Sm-Nd isotopic analyses of apatite, titanite, monazite and perovskite using LA-MC-ICPMS.

data straddle an isochron at 190 Ma (Figure 4(b-1)). The $^{145}\text{Nd}/^{144}\text{Nd}$ value of 0.348414 ± 34 (2SD) is identical to the recommended one, suggesting that our data are reli-

able (Figure 4(b-2)). With a formation age of 190 Ma, the average $\epsilon_{\text{Nd}}(t)$ value of 25 analyses is 1.7 ± 0.8 (2SD), agreeing well with the values obtained from the

whole-rocks.

Monazite (BY1 and BY49). Both samples were collected from the Bayan Obo giant REE-Nb-Fe deposit, with BY1 collected from a carbonatitic dyke intruded into the quartz conglomerate of Meso-Proterozoic Bayan Obo Group. Zircon U-Pb analyses indicate that this dyke was emplaced at ~1.4 Ga, but underwent alteration at a later stage^[23]. At 20 μm and 6 Hz, thirty-three analyses indicated that there is significant variation in the $^{147}\text{Sm}/^{144}\text{Nd}$ and $^{143}\text{Nd}/^{144}\text{Nd}$ ratios. With two exceptions, the remaining 31 analyses yield an isochron age of 1.32 ± 0.21 Ga, same as the zircon U-Pb age, within errors. The initial $^{143}\text{Nd}/^{144}\text{Nd}$ ratio is 0.510885 ± 58 (Figure 4(c-1)) with $\varepsilon_{\text{Nd}}(t)$ of 0.67 ± 0.94 (2SD), indicating its derivation from primitive mantle.

Monazite BY49 was collected from a dolomite, the host rock of the REE mineralization, at the 1474 m level in the eastern orebody of the Bayan Obo deposit; the host dolomite is relatively pure, with weak REE mineralization. In contrast to BY1, monazite BY49 shows high $^{147}\text{Sm}/^{144}\text{Nd}$ and $^{143}\text{Nd}/^{144}\text{Nd}$ ratios (Figure 4(c-1)). At 10–20 μm and 3–6 Hz, thirty-eight analyses, with two exceptions (high $^{147}\text{Sm}/^{144}\text{Nd}$ ratios), yield an isochron of 0.86 ± 0.10 Ga; the corresponding initial $^{143}\text{Nd}/^{144}\text{Nd}$ ratio is 0.511136 ± 38 (Figure 4(c-1)). The calculated $\varepsilon_{\text{Nd}}(t)$ values are -7.7 ± 0.7 (2SD) and 2.0 ± 0.9 (2SD), respectively, if we assume that it was formed at 860 or 1400 Ma.

The above monazite analyses indicate that the Bayan Obo deposit is heterogeneous in terms of Nd isotopes. It is noted that the monazite from the dolomite might have undergone late stage alteration, which might be the reason that we cannot get an acceptable age for this deposit from the Sm-Nd and Th-Pb systems. Considering that the ablation size was only 10–20 μm in our study, it is believed that more *in situ* analyses might answer this question in the future.

Perovskite (MY12). This sample was collected from the Mengyin kimberlite in Shangdong Province, China. It is a groundmass mineral, but crystallized from kimberlitic magma at an early stage^[24]. The average $^{147}\text{Sm}/^{144}\text{Nd}$ and $^{143}\text{Nd}/^{144}\text{Nd}$ ratios of 15 measurements with a spot size of 60 μm (4 Hz) were 0.0664 ± 21 (2SD) and 0.512229 ± 40 (2SD) (Figure 4(d-1)), respectively, indicating its narrow variation. Additionally, the average $^{145}\text{Nd}/^{144}\text{Nd}$ ratio was 0.348419 ± 28 (2SD) (Figure 4(d-2)), which agrees well with the recommended value.

The average $^{147}\text{Sm}/^{144}\text{Nd}$ and $^{143}\text{Nd}/^{144}\text{Nd}$ ratio of two aliquots measured by isotope dilution were 0.0686, 0.0673 and 0.512225 ± 12 (2 σ), 0.512235 ± 14 (2 σ), which are identical to those obtained by laser ablation analysis. Assuming a crystallization age of 470 Ma, the obtained average $\varepsilon_{\text{Nd}}(t)$ value is -0.16 ± 0.78 (2SD), indicating that the Mengyin kimberlite was derived from a primitive mantle.

5 Discussions

From the measurement of several minerals, it has been shown that reliable Nd isotopic data can be obtained by LA-MC-ICP-MS. However, we have to overcome two problems in its practical application; the Sm/Nd ratios suitable for correcting the isobaric interference of ^{144}Sm on ^{144}Nd , and the minimal Nd concentrations for laser ablation analysis.

For the former, we can define this from the measurement of Nd isotopes for standard glass NIST 610 in the Neptune ICP-MS. According to previous research, the concentrations of Sm and Nd for this standard glass are approximately 441–460 and 429–442 ppm^[25], respectively, and the $^{143}\text{Nd}/^{144}\text{Nd}$ ratio is 0.511927 ± 4 (2SD, $n = 4$)^[26] or 0.511908 ± 4 (2SD, $n = 3$)^[11]. Therefore, the Sm/Nd ratio of NIST 610 is approximately 1.04, corresponding to 0.6277 ± 1 (2SD, $n=3$) of $^{147}\text{Sm}/^{144}\text{Nd}$ ratio^[11]. The average $^{147}\text{Sm}/^{144}\text{Nd}$ and $^{143}\text{Nd}/^{144}\text{Nd}$ ratios of 15 measurements with the spot sizes of 60 μm (8 Hz) and 80 μm (10 Hz) were 0.6551 ± 26 (2SD) and 0.511910 ± 77 (2SD) (Figure 5), respectively, with a $^{145}\text{Nd}/^{144}\text{Nd}$ ratio of 0.348404 ± 74 (2SD). These measurements indicate that reliable $^{143}\text{Nd}/^{144}\text{Nd}$ ratio data can still be obtained even when the Sm/Nd is clear to 1.

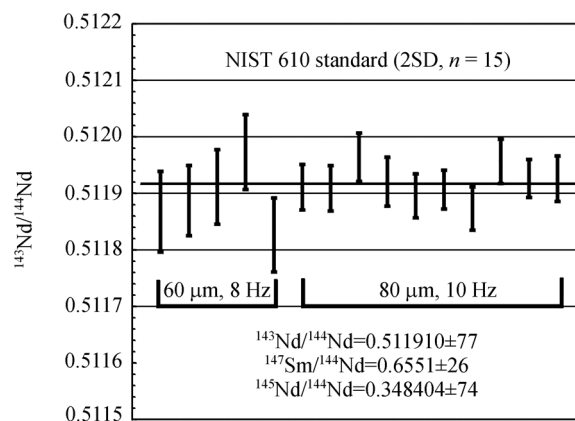


Figure 5 Nd isotopic composition of NIST 610 standard glass by laser ablation analyses.

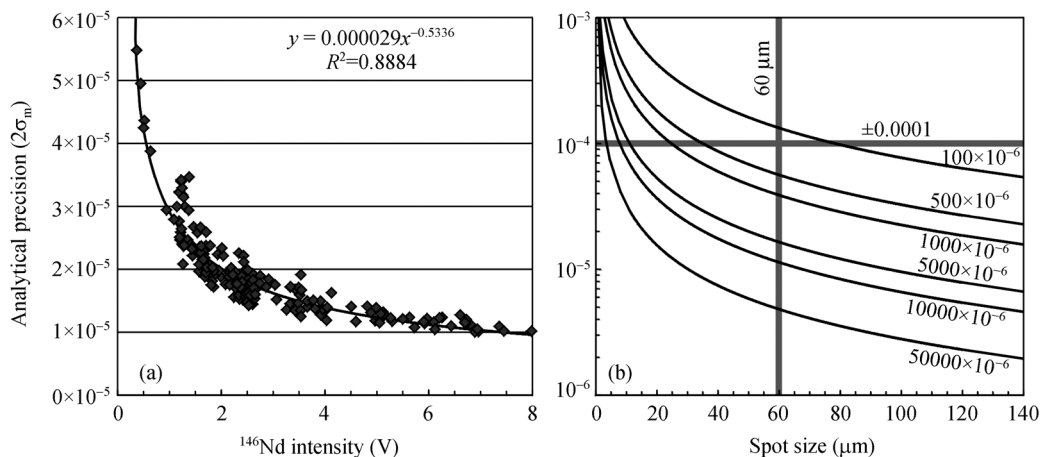


Figure 6 Relationship between Nd concentration of geological materials and measurement precision during laser ablation analyses.

However, the deviation of $^{147}\text{Sm}/^{144}\text{Nd}$ ratio is approximately 4% because of mass calibration. Therefore, reliable *in situ* Sm-Nd isotopic data can be obtained for high Nd concentration samples by the LA-MC-ICPMS technique, considering that the $^{147}\text{Sm}/^{144}\text{Nd}$ ratio of most natural geological materials is approximately 0.1.

For the Nd concentration requirement for laser ablation analysis, we can see from Figure 6 that the relationship between signal intensity and measurement deviation can be described as a function based on our previous data for apatite, titanite and perovskite (Figure 6(a)). According to the established relationship, the data precision under different laser spot sizes is governed by the Nd concentration (Figure 6(b)). The higher the Nd concentration of the samples, the larger the laser spot size or higher pulse repetition, the higher the signal intensity and precision of the $^{143}\text{Nd}/^{144}\text{Nd}$ ratio. If the deviation requirement in practical geological application is $\pm 2\varepsilon$ unit, correspondingly the $^{143}\text{Nd}/^{144}\text{Nd}$ ratio deviation will be approximately 0.0001. Under this situation, the minimal Nd concentration of a sample is approximately 200 ppm using a 60 μm laser spot size and 8 Hz repetition. It is evident that the Nd concentration required for laser analysis will reduce with future technique development. Therefore, reliable *in situ* Nd isotope data can be obtained by current techniques for REE-enriched minerals like apatite, titanite, allanite, xenotime, fluorite, monazite and perovskite; though this technique is not available for most geological materials with normal Nd concentration. In particular, for LREE-enriched mona-

zite, enough precision can be obtained even using 5–10 μm laser spot size and 8 Hz repetition. Considering that the above mentioned minerals occur widely in nature, and have been selected as important in geochemistry and geochronology^[27], the *in situ* Nd isotope measurement by laser ablation will play an important role in solid earth sciences in the future.

6 Conclusions

(1) It is shown that the mass biases of Sm and Nd are different and change with time during *in situ* Nd isotope analysis using a Neptune MC-ICPMS, coupled with a Geolas 193 nm ArF excimer laser.

(2) For relatively high Nd concentrations in geological materials, such as apatite, titanite, monazite and perovskite, reliable $^{143}\text{Nd}/^{144}\text{Nd}$ and $^{147}\text{Sm}/^{144}\text{Nd}$ ratios can be obtained using the *in situ* LA-MC-ICPMS method by applying the newly-determined Sm isotopic abundances to correct the isobaric interference of ^{144}Sm on ^{144}Nd .

(3) Spatial resolution is governed by the Nd concentration of samples during laser ablation analysis and reliable Nd isotopic data can be obtained using 5 μm spot size for REE-enriched minerals like monazite, which provides an important new technique for the determination of sub-grain Nd isotopic values.

Dr. Qiu Zhili is thanked for providing Afghanistan apatites. Constructive comments from two anonymous reviewers have substantially improved the final paper.

1 Faure G, Mensing T M, *Isotopes: Principles and Applications*. 3rd ed.. New Jersey: John Wiley & Sons, 2005. 75–112, 436–451

2 Chen F K, Hegner E, Todt W, Zircon ages, Nd isotopic and chemical compositions of orthogneisses from the Black Forest, Germany-

- evidence for a Cambrian magmatic arc. *Int J Earth Sci*, 2000, 88: 791–802[DOI]
- 3 Halliday A N, Lee D C, Christensen J N, et al. Recent developments in inductively coupled plasma magnetic sector multiple collector mass spectrometry. *Int J Mass Spectrom Ion Proc*, 1995, 146/147: 21–33[DOI]
 - 4 Halliday A N, Lee D C, Christensen J N, et al. Applications of multiple collector-ICPMS to cosmochemistry, geochemistry, and paleoceanography. *Geochim Cosmochim Acta*, 1998, 62: 919–940[DOI]
 - 5 Luais B, Telouk P, Albarede F. Precise and accurate neodymium isotopic measurements by plasma-source mass spectrometry. *Geochim Cosmochim Acta*, 1997, 61: 4847–4854[DOI]
 - 6 Vance D, Thirlwall M. An assessment of mass discrimination in MC-ICPMS using Nd isotopes. *Chem Geol*, 2002, 185: 227–240[DOI]
 - 7 Liang X R, Wei G J, Li X H, et al. Precise measurement of $^{143}\text{Nd}/^{144}\text{Nd}$ and Sm/Nd ratios using multiple collectors inductively coupled plasma mass spectrometer (MC-ICPMS). *Geochimica* (in Chinese with English abstract), 2003, 32(1): 91–95
 - 8 Yang Y H, Zhang H F, Xie L W, et al. Accurate measurement of neodymium isotopic composition using Neptune multiple collector inductively coupled plasma mass spectrometry. *Chin J Anal Chem.*, 2007, 35(1): 71–74
 - 9 He X X, Tang S H, Zhu X K, et al. Precise measurement of Nd isotopic ratios by means of multi-collector magnetic sector inductively coupled plasma mass spectrometry. *Acta Geosci Sin* (in Chinese with English abstract), 2007, 28: 405–410
 - 10 Rehkamper M, Schonbachler M, Stirling C H, Multiple collector ICP-MS: introduction to instrumentation, measurement techniques and analytical capabilities. *Geostand Newsl*, 2001, 25: 23–40[DOI]
 - 11 Foster G L, Vance D, *In situ* Nd isotopic analysis of geological materials by laser ablation MC-ICP-MS. *J Anal Atomic Spectro*, 2006, 21: 288–296[DOI]
 - 12 Foster G L, Carter A, Insights into the patterns and locations of erosion in the Himalaya—A combined fission-track and in situ Sm–Nd isotopic study of detrital apatite. *Earth Planet Sci Lett*, 2007, 257: 407–418[DOI]
 - 13 McFarlane C R M, McCulloch M T, Coupling of *in-situ* Sm–Nd systematics and U–Pb dating of monazite and allanite with applications to crustal evolution studies. *Chem Geol*, 2007, 245: 45–60[DOI]
 - 14 Xu P, Wu F Y, Xie L W, Yang Y H, Hf isotopic compositions of the standard zircons for U–Pb dating. *Chin Sci Bull*, 2004, 49: 1642–1648
 - 15 Wu F Y, Yang Y H, Xie L W, et al. Hf isotopic compositions of the standard zircons and baddeleyites used in U–Pb geochronology. *Chem Geol*, 2006, 234: 105–126[DOI]
 - 16 Ramos F C, Wolff J A, Tollstrup D L. Measuring $^{87}\text{Sr}/^{86}\text{Sr}$ variation in minerals and groundmass from basalts using LA- MC-ICPMS. *Chem Geol*, 2004, 211: 135–158[DOI]
 - 17 Dubois J C, Retali G, Cesario J, Isotopic analysis of rare earth elements by total vaporization of samples in thermal ionization mass spectrometry. *Int J Mass Spectrom Ion Process*, 1992, 120: 163–177[DOI]
 - 18 Isnard H, Brennetot R, Caussignac C, Caussignac N, Chartier F, Investigations for determination of Gd and Sm isotopic compositions in spent nuclear fuels samples by MC ICPMS. *Int J Mass Spectro*, 2005, 246: 66–73[DOI]
 - 19 Woodhead J, Hergt J, Shelley M, Eggins S, Kemp R, Zircon Hf-isotope analysis with an excimer laser, depth profiling, ablation of complex geometries, and concomitant age estimation. *Chem Geol*, 2004, 209: 121–135[DOI]
 - 20 Yuan H L, Gao S, Dai M N, et al. Simultaneous determinations of U–Pb age, Hf isotopes and trace element compositions of zircon by excimer laser ablation quadrupole and multiple collector ICP-MS. *Chem Geol*, 2008, 247: 100–118
 - 21 Wasserburg G J, Jacobsen S B, DePaolo D J, et al. Precise determination of Sm/Nd ratios, Sm and Nd isotopic abundances in standard solutions. *Geochim Cosmochim Acta*, 1981, 45: 2311–2323[DOI]
 - 22 Sun D Y, Wu F Y, Lin Q, et al. Petrogenesis and crust-mantle interaction of early Yanshanian Baishishan pluton in Zhanguangcai Ranges. *Acta Petrol Sin* (in Chinese with English abstract), 2001, 17: 227–235
 - 23 Fan H R, Hu F F, Chen F K, et al. Intrusive age of No. 1 carbonatite dyke from Bayan Obo REE–Nb–Fe deposit, Inner Mongolia: with answer to comment of Dr. Le Bas. *Acta Petrol Sin* (in Chinese with English abstract), 2006, 22: 519–520
 - 24 Chi J S, Lu F X. Kimberlites and the Features of Paleozoic Lithospheric Mantle in North China Craton (in Chinese with English summary). Beijing: Science Press, 1996. 292
 - 25 Rocholl A, Dulski P, Raczek I, New ID-TIMS, ICP-MS and SIMS data on the trace element composition and homogeneity of NIST certified reference material SRM 610-611. *Geostand Newsl*, 2000, 24: 261–274[DOI]
 - 26 Woodhead J D, Hergt J M. Strontium, Neodymium and Lead isotope analyses of NIST glass certified reference materials: SRM 610, 612, 614. *Geostand Newsl*, 2001, 25(2-3): 261–266[DOI]
 - 27 Poitrasson F, Hanchar J M, Schaltegger U. The current state and future of accessory mineral research. *Chem Geol*, 2002, 191: 3–24[DOI]